

## Supplementary Materials for

### **SWI/SNF blockade disrupts PU.1-directed enhancer programs in normal hematopoietic cells and acute myeloid leukemia**

Courtney Chambers<sup>1,2</sup>, Katerina Cermakova<sup>1</sup>, Yuen San Chan<sup>1</sup>, Kristen Kurtz<sup>3</sup>,  
Katharina Wohlan<sup>3</sup>, Andrew Henry Lewis<sup>4</sup>, Christiana Wang<sup>5</sup>, Anh Pham<sup>6</sup>, Milan Dejmek<sup>7</sup>,  
Michal Sala<sup>7</sup>, Mario Loeza Cabrera<sup>1</sup>, Rogelio Aguilar<sup>8</sup>, Radim Nencka<sup>7</sup>, H. Daniel Lacorazza<sup>4</sup>,  
Rachel E. Rau<sup>3,8\*</sup>, H. Courtney Hodges<sup>1,6,9\*</sup>

<sup>1</sup> Department of Molecular and Cellular Biology, Center for Precision Environmental Health, and Dan L Duncan Comprehensive Cancer Center, Baylor College of Medicine, Houston, TX, 77030, USA

<sup>2</sup> Translational Biology and Molecular Medicine Graduate Program, Houston, TX, 77030, USA

<sup>3</sup> Department of Pediatrics, Baylor College of Medicine and Texas Children's Hospital, Houston, TX, 77030, USA

<sup>4</sup> Department of Pathology and Immunology, Baylor College of Medicine, Houston, TX, 77030, USA

<sup>5</sup> Genetics and Genomics Graduate Program, Baylor College of Medicine, Houston, TX, 77030, USA

<sup>6</sup> Department of Bioengineering, Rice University, Houston, TX, 77005, USA

<sup>7</sup> Institute of Organic Chemistry and Biochemistry of the Czech Academy of Sciences, Prague, 160 00, Czech Republic

<sup>8</sup> Stem Cells and Regenerative Medicine Center, Baylor College of Medicine, Houston, TX, 77030, USA

<sup>9</sup> Center for Cancer Epigenetics, The University of Texas MD Anderson Cancer Center, Houston, TX, 77030, USA

\* Corresponding author.

Rachel E. Rau (R.E.R.)

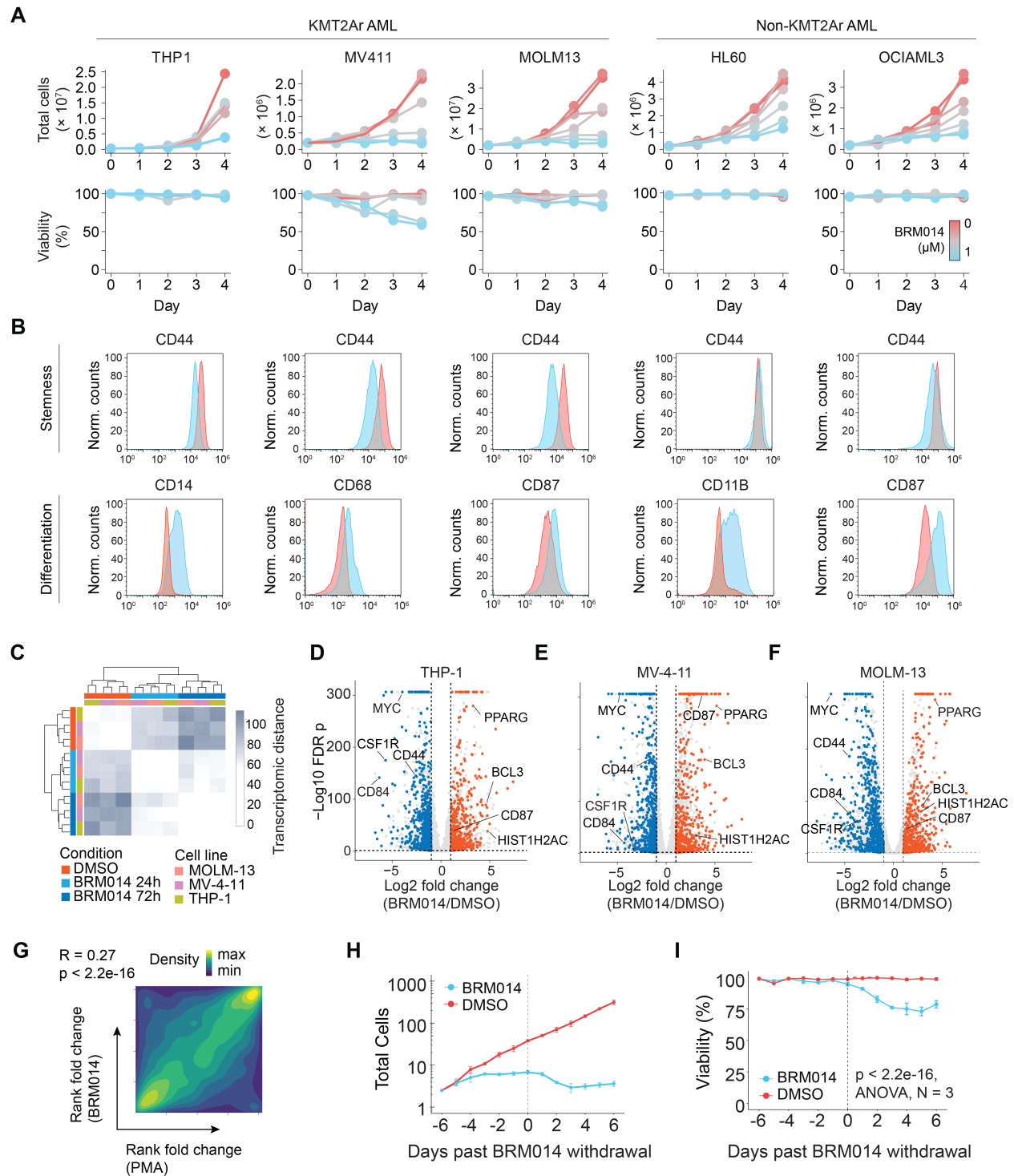
1 Baylor Plaza, Houston, TX 77030

E-mail: rachel.rau@bcm.edu

H. Courtney Hodges (H.C.H.)

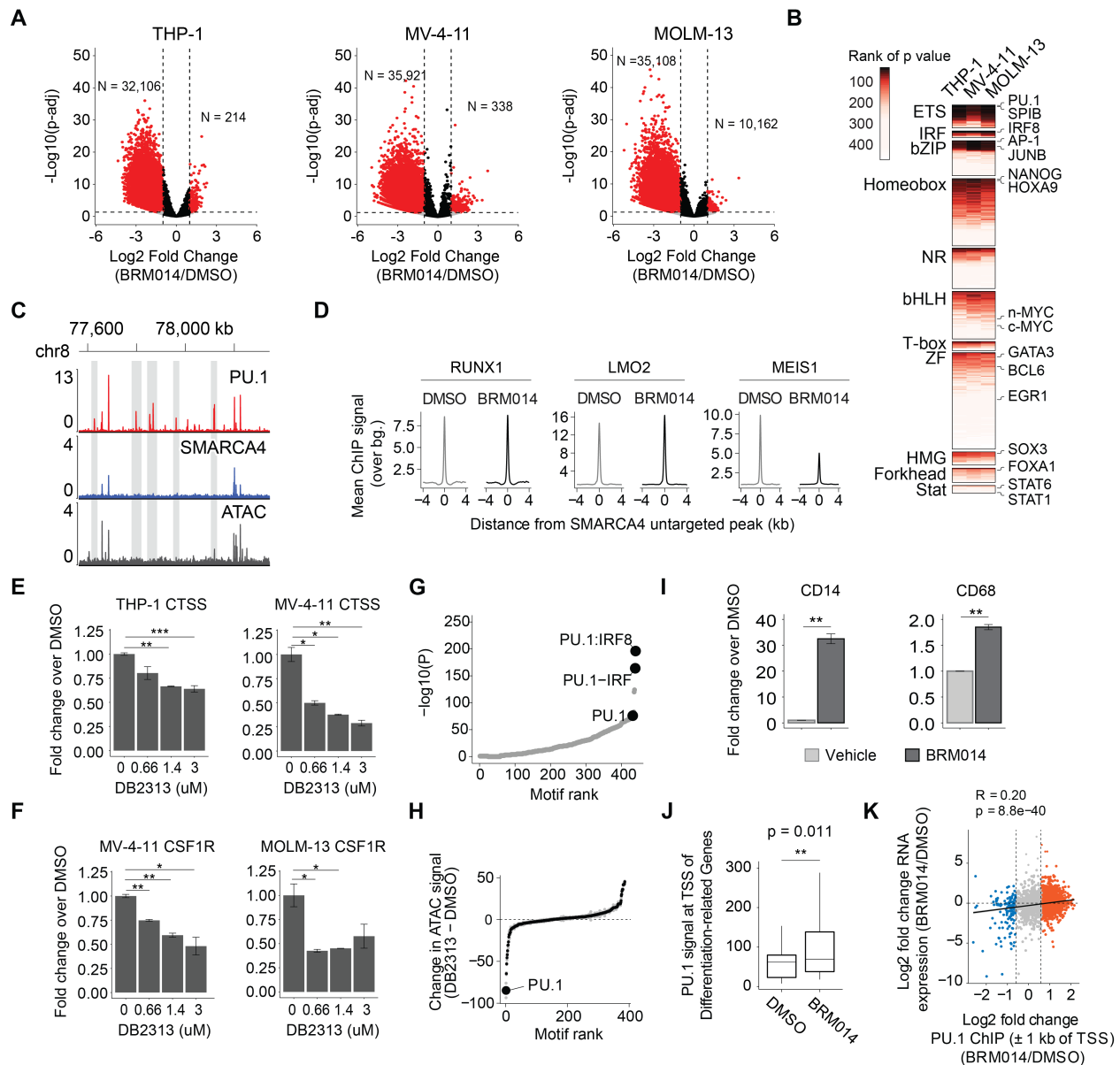
1 Baylor Plaza, Houston, TX 77030

E-mail: chodges@bcm.edu



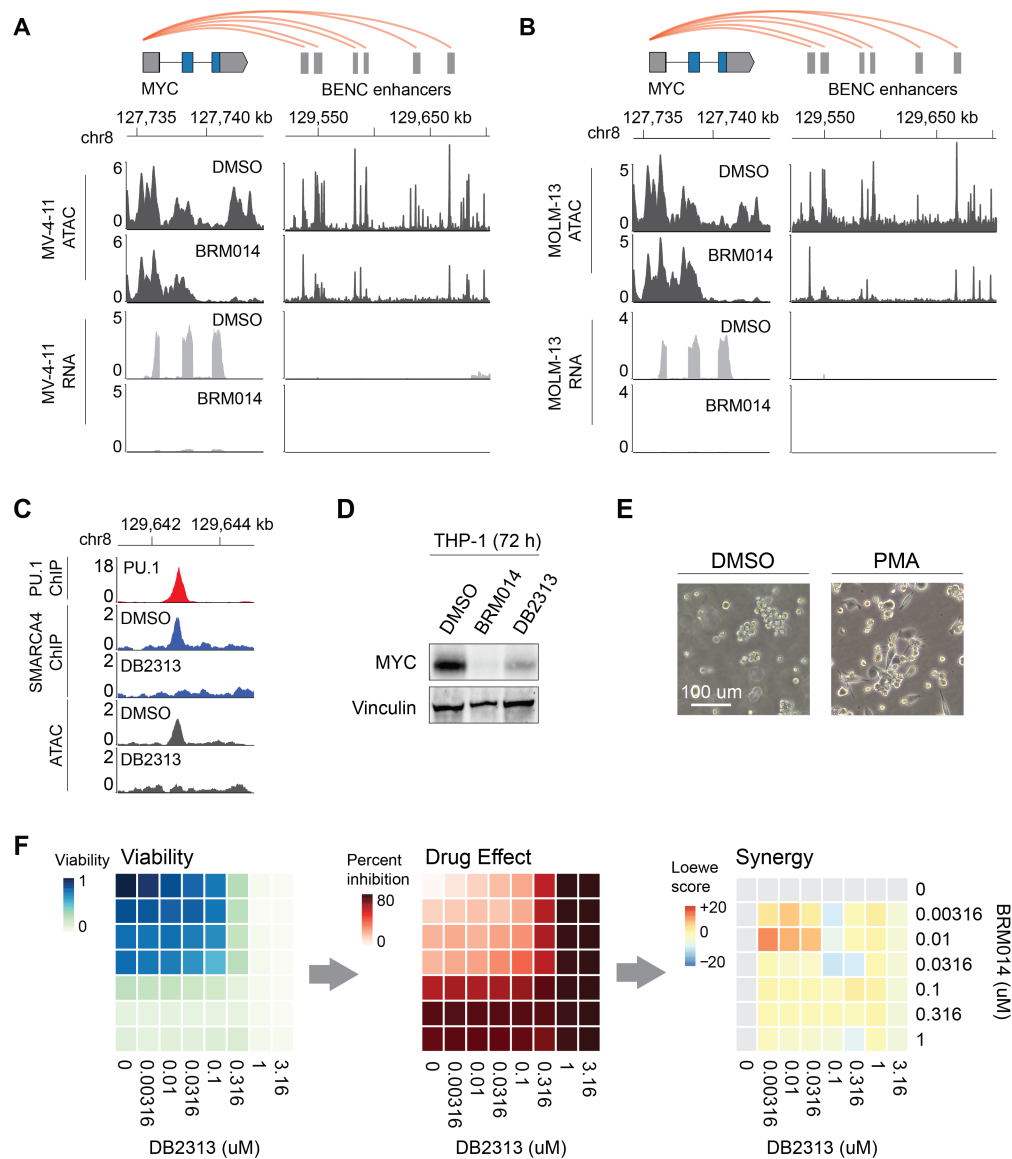
**Supplementary Figure S1. SWI/SNF inhibition causes loss of proliferation and myeloid differentiation in AML.** (A) Proliferation (top), viability (bottom), and (B) flow cytometry analysis at 72 h of stemness and myeloid differentiation cell surface markers in AML cell lines treated with BRM014. (C) Unbiased clustering of AML cell lines treated with BRM014 or DMSO control based on RNA-seq. The resulting clustering by treatment duration indicates that BRM014 has a similar effect across AML cell lines. (D) Gene expression changes induced by treatment with

1  $\mu$ M BRM014 for 72 h in THP-1, **(E)** MV-4-11, and **(F)** MOLM-13 cell lines measured by RNA-seq. Transcripts significantly upregulated by BRM014 across all cell lines are shown in red, and transcripts downregulated across all cell lines are shown in blue. Significance threshold absolute Log<sub>2</sub> Fold Change  $\geq 1$  with  $p < 0.05$ . **(G)** Genome-wide correlation of BRM014- and PMA-induced transcriptional changes in THP-1 cells based on RNA-seq. The strong correlation indicates that BRM014 and PMA result in similar gene expression changes. **(H)** Proliferation and **(I)** viability of THP-1 cells treated with 1  $\mu$ M BRM014 for 6 days and monitored for 6 days after drug withdrawal measured by trypan blue. Cells remain cytostatic after removal of drug, demonstrating that prolonged exposure to BRM014 results in irreversible growth arrest. Error bars: mean  $\pm$  SEM for N = 3.



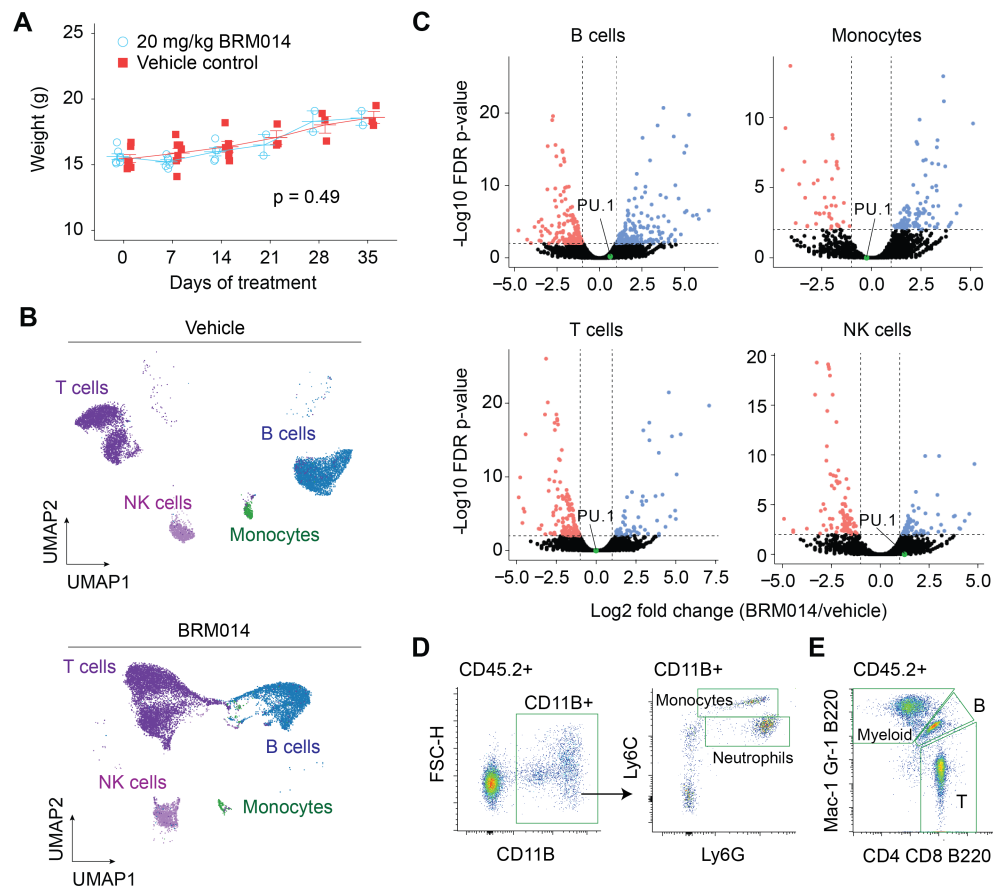
**Supplementary Figure S2. Genome-wide chromatin features underlying response to BRM014 and DB2313.** (A) DNA accessibility changes induced by treatment with BRM014 for 72 h in AML cell lines at SMARCA4-occupied sites measured by ATAC-seq. (B) Ranked TF motifs that lose accessibility after treatment with BRM014 in AML cell lines measured by ATAC-seq. Motifs are clustered by family and TFs related to hematopoiesis and differentiation are highlighted. (C) Representative browser track of PU.1 binding in AML cells. Inaccessible sites bound by PU.1 and not occupied by SMARCA4 highlighted. (D) CRC TF binding at sites unbound by SMARCA4 in THP1 cells treated with BRM014 versus DMSO. (E) Reduced expression of known PU.1 targets *CTSS* and (F) *CSF1R* in AML cells treated with a serial titration of DB2313, measured by RT-qPCR, N=2 per condition. (G) Ranking of motifs associated with decreased SMARCA4 binding in THP-1 cells treated with 3  $\mu\text{M}$  DB2313 versus DMSO control. (H) Ranking of differential TF motif accessibility in THP-1 cells treated with DB2313 versus DMSO control. (I) Expression of myeloid differentiation genes *CD14* and *CD68* upon BRM014 treatment

measured by RNA-seq. **(J)** PU.1 occupancy at the TSS of differentiation-related genes in THP-1 cells treated with BRM014 or DMSO control. See Methods for details. **(K)** Correlation between BRM014-induced PU.1 occupancy and gene expression changes. Error bars: mean  $\pm$  SEM. \* $p < 0.05$ , \*\* $p < 0.01$ , \*\*\* $p < 0.001$ .

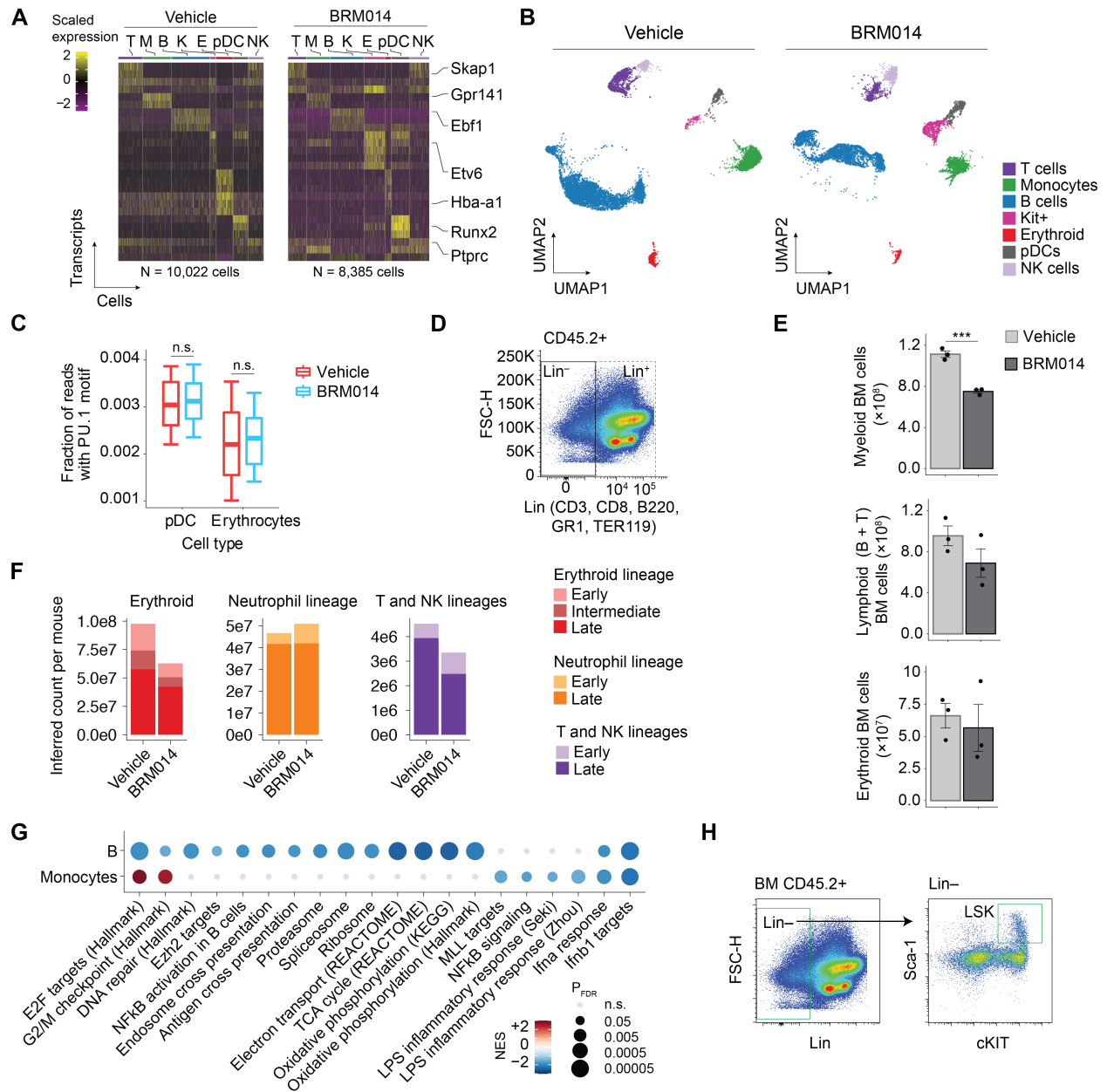


**Supplementary Figure S3. Convergence of SWI/SNF and PU.1 activity on MYC expression and drug response.** Browser tracks of chromatin accessibility and gene expression in BRM014- and DMSO-treated **(A)** MV-4-11 and **(B)** MOLM-13 at *MYC* and BENC measured by ATAC-seq and RNA-seq, respectively. **(C)** Representative browser track of SMARCA4 binding at a PU.1 site in BENC upon DB2313 treatment. **(D)** MYC expression in THP-1 cells treated with BRM014 or DB2313 for 72 h. **(E)** Morphological changes induced by PMA-differentiation in THP-1 cells. **(F)**

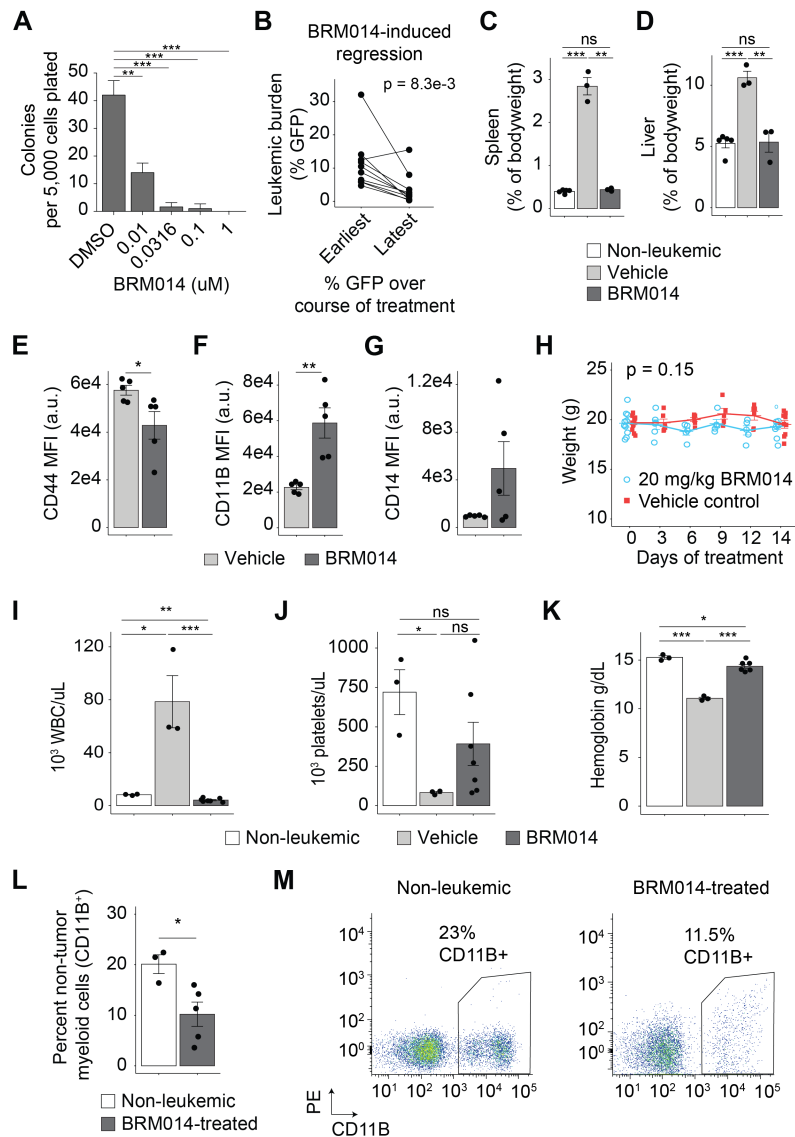
Heatmap of viability, mean inhibition, and synergy score for BRM014 and DB2313 cross-titration in THP-1 cells for N = 2.



**Supplementary Figure S4. BRM014 alters immune populations and gene expression in the peripheral blood of healthy mice.** (A) Weight of mice over the two-week treatment period, N = 11 independent mice (details in Methods). (B) UMAP embedding of individual cells (sn-multiome) from the peripheral blood of BRM014- and vehicle-treated mice. Resulting clusters are classified by immune cell type based on cell-specific expression profiles. (C) Gene expression changes induced by BRM014 in peripheral immune populations measured by scRNA-seq. (D) Gating for peripheral neutrophils (CD11B<sup>+</sup>Ly6G<sup>+</sup>) and monocytes (CD11B<sup>+</sup>Ly6C<sup>+</sup>). (E) Gating for peripheral B cells, T cells, and myeloid cells. Error bars: mean ± SEM.



**Supplementary Figure S5. Analysis of bone marrow from healthy BRM014- and vehicle-treated mice.** (A) Sn-multiome transcriptional profiles of bone marrow by cell type. T = T cells, M = monocytes, B = B cells, K = *KIT*<sup>+</sup> progenitors, E = erythroid cells, DC = plasmacytoid dendritic cells, NK = NK cells. (B) UMAP embedding of individual cells (sn-multiome) from the bone marrow of BRM014- and vehicle-treated mice. Resulting clusters are classified by immune cell type based on cell-specific expression profiles. (C) Quantification of accessible PU.1 motifs across specific cell types. (D) Gating of lineage-committed versus uncommitted BM cells. (E) Total number of myeloid, lymphoid, and erythroid cells in bone marrow at day 14 measured by flow cytometry, N = 3 per condition. (F) Inferred total number of B cell and monocyte populations in BM determined by scRNA-seq. (G) Lineage-specific effects on B cells and monocytes from BRM014- versus DMSO-treated mice by GSEA. (H) Gating for LSK (Lin<sup>-</sup>Sca-1<sup>+</sup>cKit<sup>+</sup>) HSPCs within bone marrow. Error bars: mean ± SEM. \*p < 0.05, \*\*p < 0.01, \*\*\*p < 0.001.



**Supplementary Figure S6. Effect of SWI/SNF inhibition on peripheral immune populations in leukemic mice.** (A) Number of colonies formed by murine MLL-AF9 cells treated with a serial titration of BRM014 or DMSO control in vitro, N = 3 per condition. (B) Peripheral leukemic burden of BRM014-treated mice at their earliest and latest blood collection time points during the 2-week treatment period. Weight of (C) spleens and (D) livers harvested from BRM014- or vehicle-treated mice compared to non-leukemic controls, N = 5 (non-leukemic), N = 3 (vehicle), N = 3 (BRM014). Expression of (E) CD44 ( $p = 0.03$ ) and (F) CD11B ( $p = 0.04$ ) and (G) CD14 on peripheral leukemic GFP<sup>+</sup> cells from mice treated with BRM014 or vehicle control for 9 days, N = 5 per condition. (H) Weight of mice over the two-week treatment period, N = 11 (vehicle) and N = 10 (BRM014), details in Methods. (I) White blood cell (WBC), (J) platelet, and (K) hemoglobin levels of BRM014-treated, vehicle-treated, and non-leukemic control mice 3 days after completion of treatment course, N = 3 (non-leukemic), N = 3 (vehicle), N = 7 (BRM014). (L) Percent of non-tumor myeloid (CD11B<sup>+</sup>) cells in the peripheral blood of BRM014-treated mice at day 9 compared to a non-leukemic reference mouse and (M) representative flow plots. Cells in



L and M were gated based on GFP<sup>-</sup> cells, N = 3 (non-leukemic), N = 5 (BRM014). Error bars: mean ± SEM. \*p < 0.05, \*\*p < 0.01, \*\*\*p < 0.001.

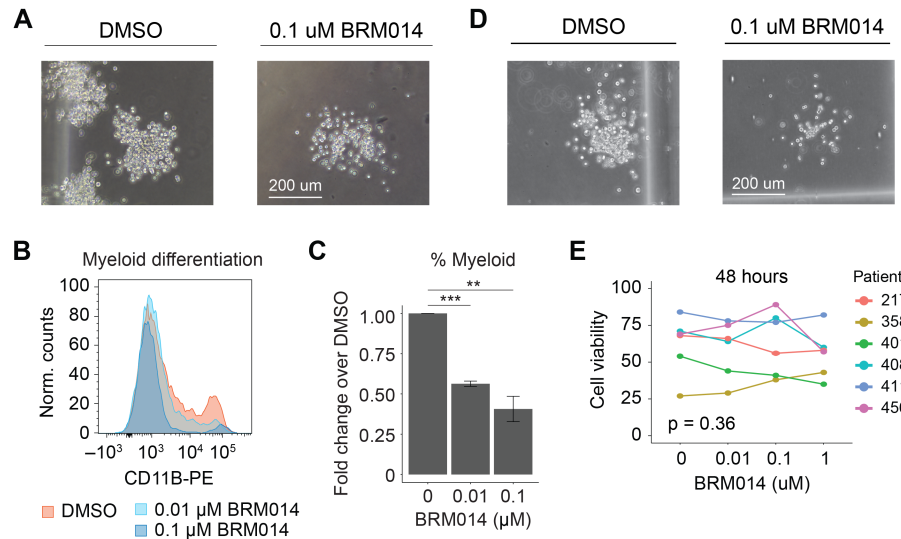


**Figure S7. SWI/SNF inhibition is effective in primary human cells and suppresses myeloid differentiation capacity of CD34<sup>+</sup> HSPC progenitors.** (A) Representative images of myeloid colonies formed by CD34<sup>+</sup> cells treated with 0.1 uM BRM014 or DMSO control. (B) Histogram and (C) quantification of CD11B<sup>+</sup> myeloid cells differentiated from CD34<sup>+</sup> cells treated with BRM014 or DMSO control measured by flow cytometry, N = 3. (D) Representative images of colonies formed by leukemia cells from donor 408 treated with 0.1 uM BRM014 or DMSO control. (E) Viability of primary leukemic blasts treated with a serial titration of BRM014 or DMSO control in liquid culture for 48 hours. Error bars: mean ± SEM. \*p < 0.05, \*\*p < 0.01, \*\*\*p < 0.001.

## Supplemental Datasets

**Supplemental Dataset 1. RNA-seq datasets.** Summary data for all RNA-seq data sets described in this work. Includes MOLM-13, MV-4-11, and THP-1. Treatments include BRM014, PMA, or DMSO control. Excel spreadsheet.

**Supplemental Dataset 2. Gene set enrichment analyses.** Summary results for gene set enrichment analysis (GSEA) corresponding to RNA-seq data. Includes MOLM-13, MV-4-11, and THP-1 cells treated with BRM014 for 72 h compared to DMSO control. Excel spreadsheet.

**Supplemental Dataset 3. Motif profiling.** Summary results for transcription factor motif profiling corresponding to ATAC-seq data. Includes MOLM-13, MV-4-11, and THP-1 cells treated with BRM014 for 72 h compared to DMSO control. Excel spreadsheet.

**Supplemental Dataset 4. Complete blood counts.** Summary data for complete blood count (CBC) data in mice treated with either BRM014 or vehicle control three days after termination of treatment. Excel spreadsheet.

## Supplemental Methods

### Preparation of BRM014

**Synthesis.** BRM014 was synthesized as described earlier (1) with minor changes described below. In particular, the phenyl (5-(((TBDMS)oxy)methyl)-2-fluoropyridin-4-yl)carbamate was prepared according to the published protocol, with the exception of the fluorination step, which was carried out with CsF instead of TMAF. This approach resulted in slightly lower yield but allowed us to use more accessible reagent. The 3-(difluoromethyl)isothiazol-5-amine was also prepared according to the published procedure with only minor adjustment. Borane dimethylsulfate complex was used instead of borane-THF complex. The coupling conditions used for the merging of these two fragments were optimized: longer reaction time at lower temperature was used in the LiHMDS-mediated reaction and HF-TEA was employed in the final deprotection, which resulted in doubling of the overall yield of the final compound. The final synthesized product was either crystallized or lyophilized prior to reconstitution in DMSO. Final crystallization helped remove residual color in the BRM014 and resulted in colorless needles. Both lyophilized and crystallized products were determined to have equivalent biological activity.

**Validation and quality control.** To assess the quality and purity of the synthesized BRM014,  $^{19}\text{F}$  and  $^1\text{H}$  NMR spectra were recorded on a Bruker Avance III HD 400 MHz using solvent signal as a reference. Identity of the BRM014 structure was verified by measuring  $^{13}\text{C}$ , H,C-HSQC and H,C-HMBC spectra using standard pulse programs from the library of the spectrometer. Gradient selection was used in the 2D experiments, and all signals were assigned to their respective atoms.  $^1\text{H}$  NMR (400 MHz, DMSO- $d_6$ )  $\delta$  11.76 and 9.25 (bs, 1H, NH), 8.05 (s, 1H, H-5), 7.77 (s, 1H, H-2), 7.09 (s, 1H, H-4'), 6.95 (t, 1H,  $J_{\text{H,F}} = 54.4$  Hz,  $\text{CHF}_2$ ), 5.72 (t, 1H,  $J_{\text{OH,CH}_2} = 5.1$  Hz, OH), 4.59 (s, 2H,  $J_{\text{CH}_2,\text{OH}} = 4.4$  Hz,  $\text{CH}_2\text{O}$ ).  $^{13}\text{C}$  NMR (101 MHz, DMSO- $d_6$ )  $\delta$  163.70 (H-5'), 163.64 (d,  $J_{1,\text{F}} = 230.3$  Hz, C-1), 159.04 (t,  $J_{3',\text{F}} = 26.8$  Hz, C-3'), 152.25 (C=O), 148.94 (d,  $J_{3,\text{F}} = 12.5$  Hz, C-3), 146.55 (d,  $J_{5,\text{F}} = 17.9$  Hz, C-5), 123.04 (d,  $J_{4,\text{F}} = 3.7$  Hz, C-4), 111.53 (t,  $J_{\text{C-F}} = 237.1$  Hz,  $\text{CHF}_2$ ), 104.03 (C-4'), 97.66 (d,  $J_{2,\text{F}} = 45.2$  Hz, C-2), 58.59 ( $\text{CH}_2\text{O}$ ).  $^{19}\text{F}$  NMR (470.4 MHz, DMSO- $d_6$ )  $\delta$  -69.98 (s), -113.82 (d,  $J = 54.5$  Hz). Additionally, LC-MS analysis was performed using a Waters UPLC H-Class Core System, UPLC PDA detector and Mass spectrometer Waters SQD2. For all materials used in this study, the expected molecular weight of 318 Da was confirmed, and purity of >99% was confirmed based on LC-MS measurement.

### Inhibitor treatments

**BRM014 treatment.** BRM014 powder was reconstituted in DMSO to 10 mM and stored at -80 °C. Further dilutions in DMSO were performed to make working stocks (1000X for each desired final drug concentration), which were diluted 1:1000 in media to achieve the final desired concentration. Treatment concentrations and exposure durations are described in the method sections of each assay.

**DB2313 treatment.** DB2313 (Cat# HY-124629, MedChem Express) was reconstituted in DMSO to 10 mM and stored at -80 °C. Further dilutions in DMSO were performed to make working stocks (1000X for each desired drug concentration). For treatment, cells were seeded in triplicates at  $2 \times 10^5$

cells/mL and DB2313 working stocks were added to media at 1:1,000 to achieve the following final concentrations: 0 nM (DMSO), 660 nM, 1.4  $\mu$ M, or 3  $\mu$ M.

### Assessment of cell growth, viability, morphology, and synergy

**Proliferation and viability assays.** Cells were plated at  $2 \times 10^5$  cells/mL in 96-well plates and treated with DMSO control or BRM014 (3.16-fold serial dilutions). Cell counts and percent viability were assessed daily for 6 days using Trypan blue viability dye with a BioRad TC20 cell counter. For BRM014 withdrawal assays, cells were plated at  $2 \times 10^5$  cells/mL in 24-well plates and treated with DMSO control or 1  $\mu$ M BRM014. After the designated treatment length, cells were spun down and resuspended in BRM014/DMSO-free media. Cell proliferation and viability were assessed daily via Trypan blue and were monitored for 6 days after the drug was withdrawn.

**Microscopy.** Primary cells were plated at  $2 \times 10^5$  cells/mL and treated with DMSO control or 1  $\mu$ M BRM014 for 48. Cells were spun onto microscope slides at 300 rpm for 5 minutes and allowed to dry. Slides were stained with May-Grunwald stain (Sigma-Aldrich, MG500-500ML) for 3 minutes and then Giemsa stain (Sigma-Aldrich, GS-500) for 17 minutes. Coverslips were applied and slides were imaged at 40X using a Nikon Ts2-FL inverted microscope.

**Synergy.** For measurement of drug interactions, cells were exposed to variable concentrations of drugs for 96 hours, passaged into media containing no drugs and grown for 1 week before their proliferation capacity was assessed. Cell proliferation was assessed using alamarBlue (Cat# DAL1025, Invitrogen) according to the manufacturer's instructions. Synergy scores were determined using the synergyfinder R package. A Loewe score of  $-10 < x < 10$  is considered additive.

### Western Blotting

**Immunoblotting.** Total protein was isolated from cells using RIPA lysis buffer (50 mM Tris HCl pH 7.5, 150 mM NaCl, 1% NP-40, 0.5% sodium deoxycholate, 0.1% SDS, cOmplete ULTRA protease inhibitors (Roche)). Samples were sonicated and cleared by centrifugation, and then protein concentration was determined using the Pierce Detergent Compatible Bradford Assay Kit (Thermo Fisher). Subsequently, 30  $\mu$ g of total protein per well was run on a Novex NuPAGE 4-12% Bis Tris polyacrylamide gel in MOPS SDS running buffer (Thermo Fisher). Bands from the gel were transferred to 0.45  $\mu$ m PVDF membrane (Millipore) overnight.

**Detection.** Western blots were subsequently blocked in 5% BLOTTO (Santa Cruz) dissolved in Tris-buffered saline with 0.1% Tween 20 Detergent (TBS-T), incubated in primary antibody overnight at 4 °C, washed 3 times in TBS-T, and probed with secondary antibody for 1-2 h at RT. The following antibodies were used in this study: SMARCA4 (Santa Cruz, #sc-374197, RRID: AB\_10990135), vinculin (Cat# V9131, Sigma-Aldrich, RRID: AB\_477629), c-Myc (Cat# 5605S, Cell Signaling Technology, RRID: AB\_1903938), PU.1 (Cat# 2266S, Cell Signaling Technology, RRID: AB\_10692379), HRP conjugated mouse anti-rabbit IgG-HRP Secondary antibody (Cat# sc-2357, Santa Cruz Biolabs, RRID: AB\_628497) and StarBright Blue 520 conjugated goat anti-mouse IgG (Cat# 12005867, BioRad, RRID: RRID:AB\_324488). Detection of HRP-conjugated

antibodies was performed using Clarity Western or Clarity Max ECL substrate (Bio-Rad). Visualization was performed on a Bio-Rad ChemiDoc MP imager.

### RNA expression analysis

**RT-qPCR.** Total RNA was harvested using TRIzol reagent (Invitrogen, 15596026). cDNA was generated using a high-capacity reverse transcription kit (Fisher, 43-688-14). TaqMan real-time PCR reactions contained 1X TaqMan Fast Advanced Master Mix (Cat# 4444557, Applied Biosystems), 1X target primers (FAM-MGB), 1X housekeeping primers (VIC-MGB), and 50 ng of cDNA in a 20 uL volume. TaqMan assays used in this study are summarized in **Supplementary Table S1**. PCR was performed with a QuantStudio 3 Real-Time PCR system (Applied Biosystems) at 50 °C for 2 minutes and 95 °C for 20 seconds, followed by 40 two-step cycles of 95 °C for 1 second and 60 °C for 20 seconds. Quantification was normalized to internal TBP expression levels using the  $\Delta\Delta C_t$  method. TaqMan probe sets used in this study are provided below. For primary AML specimens, RNA was harvested after 24-hour treatment with BRM014 or DMSO control in liquid culture to assess MYC and TBP expression. One primary AML sample (301) was not analyzed for MYC expression via qPCR due to limited sample availability.

**Supplementary Table S1. TaqMan assays used in this study.**

Gene target	TaqMan assay ID	Dye label
MYC	Hs00153408_m1	FAM-MGB
MYC	Mm00487804_m1	FAM-MGB
CD14	Hs00169122_g1	FAM-MGB
CD68	Hs00154355_m1	FAM-MGB
CD44	Hs01075864_m1	FAM-MGB
CTSS	Hs00175407_m1	FAM-MGB
CSF1R	Hs00911250_m1	FAM-MGB
TBP	Hs00427620_m1	VIC-MGB
TBP	Mm01277042_m1	VIC-MGB

### Flow cytometry

**Antibody staining.** Single-cell suspensions in FACS sample buffer (1X PBS, 2% heat-inactivated FBS) were incubated with antibodies for 20 min at 4 °C. Where appropriate, cells were further incubated with streptavidin conjugates for 20 min. Cells were washed twice with FACS sample buffer, PI was added as a viability dye. The following human antibodies were used: CD44-APC (Clone IM7, Cat# 103012, BioLegend, RRID: AB\_312963), CD14-FITC (Cat# 367129, BioLegend, RRID: AB\_2721359), CD11B-APC (Cat# 301318, BioLegend, RRID: AB\_493017), CD68-PE (Clone Y1/82A, Cat #333807, BioLegend, RRID:AB\_1089057), CD87-PE (Clone VIM5, Cat# 336906, BioLegend, RRID:AB\_2165468), Annexin V-FITC (Cat# A9210, Sigma), and CD11B-PE (Clone ICRF44, Cat# 557321, BD Biosciences, RRID: AB\_396636). The following mouse antibodies were used: CD44-PE-Cy7 (Clone IM7, 25-0441-81, eBioscience, RRID:AB\_469622), CD11B-APC (Clone M1/70, 17-0112-81, eBioscience, RRID: AB\_469342), CD14-PE (Clone Sa2-8, 12-0141-81, eBioscience, RRID: AB\_465562), biotin mouse lineage panel (Cat# 559971, BD Biosciences, RRID: AB\_10053179), KIT-PE (Cat# 12-1171-82, eBioScience, RRID: AB\_465813), SCA-1-APC (Cat# 17-5981-83, eBioScience, RRID:

AB\_469488), CD8a-PB (Cat# MCD0828, Invitrogen, RRID: AB\_10372364), CD4-PB (Cat# 48-0042-82, Invitrogen, RRID: AB\_1272194), B220-PE-Cy7 (Cat# 25-0452-82, Invitrogen, RRID: AB\_469627), B220-PB (Cat# 103227, BioLegend, RRID:AB\_492876), GR-1-PE-Cy7 (Cat# 108416, BioLegend, RRID: AB\_313381), CD11B-PE-Cy7 (Cat# 101216, BioLegend, RRID: AB\_312799), CD45.2-APC (Cat# 109814, BioLegend, RRID: AB\_389211), Ly6C-PE-Cy7 (Cat# 560593, BD Pharmingen, RRID: AB\_1727557), CD3-PB (Cat# 48003282, Invitrogen, RRID: AB\_1272193), GR-1-PB (Cat# 48-5931-82, Invitrogen, RRID: AB\_1548788), Ter119-PB (Cat# 48592182, Invitrogen, RRID: AB\_1518808), SCA-1-FITC (Cat# 557405, BD Pharmingen, RRID: AB\_396688), KIT-APC (Cat# 17-1171-83, Invitrogen, RRID: AB\_469431), CD45.2-BUV395 (Cat# 564616, BD Horizon, RRID: AB\_2738867), CD11B-APC-Cy7 (Cat# 557657, BD Pharmingen, RRID: AB\_396772), and streptavidin secondary antibody PerCPCy5.5 (Cat# 405214, BioLegend). The following viability dyes were used: propidium iodide (Cat #P4864-10ML, Sigma Aldrich). Excitation and emission settings for each fluorophore are summarized in **Supplementary Table S2**.

**Supplementary Table S2. Flow cytometry and FACS settings.**

<b>Instrument</b>	<b>Fluorophore</b>	<b>Excitation (nm)</b>	<b>Emission (nm)</b>
AriaII	PI	355	530/30
	GFP	488	530/30
LSRII (M)	PI	355	650LP
	GFP, FITC	488	530/30
	PE	488	575/26
	APC	633	660/20
	PE-Cy7	488	780/60
	APC-Cy7	633	780/60
	PB	404	440/40
LSRII (T)	FITC	488	525/50
	APC	633	670/30
	PB	405	450/50
	BUV395	355	379/28
FACSCanto	GFP	488	530/30
	PE	488	585/42
	PE-Cy7	488	780/60
	APC	633	660/20
	APC-Cy7	633	780/60
SH800	GFP, FITC	488	525/50
	PE	488	600/60
	APC	638	665/30
	PB	405	450/50
	PE-Cy7	488	785/60

## Genome-wide analyses

**RNA library preparation.** Cells were treated with 1 uM BRM014, 3 uM DB2313, or DMSO control for 72 h. For PMA differentiation, THP-1 cells were treated with 10 nM PMA (Sigma, P1585-1MG). After 48 h, PMA-containing media was removed, and cells rested in PMA-free media for 24 h. Cells were harvested using TRIzol reagent, and mRNA was isolated by polyA enrichment, fragmented, and reverse transcribed into cDNA. Paired-end sequencing was performed on an Illumina NovaSeq 6000 (RRID:SCR\_016387).

**RNA-seq analysis.** As previously described (2), RNA-seq were mapped to the hg38 human reference genome using HISAT2 (RRID: SCR\_015530) (3). Reads with mapping quality <10 were discarded. Reads within genes were counted using HTseq (RRID: SCR\_005514) (4) and processed with DESeq2 (RRID: SCR\_015687) (5) using default parameters. Differential expression calls were defined by expression fold changes of >2-fold in either direction and FDR-adjusted p-values <0.05. For analysis of expression changes across cell lines, cell-line-specific expression was normalized using the limma R package (RRID:SCR\_010943).

**Gene set enrichment analysis.** Gene set enrichment was performed using the R package fgsea (version 1.14.0, RRID: SCR\_020938) (6). The following gene sets were used to generate enrichment plots: HALLMARK\_MYC\_TARGETS\_V1, BROWN\_MYELOID\_CELL\_DEVELOPMENT\_DN, JAATINEN\_HEMATOPOIETIC\_STEM\_CELL\_UP, RGAGGAARY\_PU1\_Q6.

**Analysis of PU.1 changes at TSS.** ChIP peak calls at TSSs were defined from -1 kb to +100 bp away from target genes. Differentiation-related genes were defined by the following gene set: MA\_MYELOID\_DIFFERENTIATION\_UP. Differential analysis was performed by paired t-test.

**Assay for transposase-accessible chromatin (ATAC) library preparation and sequencing.** To isolate nuclei, cells were resuspended in 50 uL of lysis buffer [0.1% Tween-20, 0.1% NP-40 and 0.01% digitonin in RSB buffer (10 mM Tris-HCl pH 7.5, 10 mM NaCl, 3 mM MgCl<sub>2</sub>)] and incubated on ice for 3 minutes. RSB buffer supplemented with 0.1% Tween-20 was used to wash out lysis buffer, and then nuclei were pelleted by centrifugation for 10 minutes at 500 g. For transposition, nuclei were resuspended in 50 uL of Transposition mix plus 25 uL of Tagmentation DNA buffer (2.5 µl Tagment DNA enzyme (Illumina), 25 µl of Tagmentation DNA buffer (Illumina), 0.1% Tween-20 and 0.01% Digitonin) and incubated for 30 minutes at 37 °C. A MinElute PCR purification kit (Qiagen) was used to purify the transposed DNA, and libraries were amplified by PCR with barcoded Nextera primers (Illumina) using 2X NEBNext High-Fidelity PCR Master Mix. Libraries were purified and size-selected with AMPure XP beads (Beckman Coulter) for fragments between ~100 and 1,000 bp in length according to the manufacturer's instructions.

**Genome browser tracks.** For each genome-wide analysis, bigWig files were created based on genomic coverage. Genome browser tracks were generated using PyGenomeTracks (7).

## Syngeneic MLL-AF9 mouse model

**MLL-AF9 cells.** To generate murine leukemias, Lin<sup>-</sup>Sca-1<sup>+</sup>c-Kit<sup>+</sup> (LSK) cells were purified from the bone marrow of 8-12 week old C57BL/6J mice using hematopoietic stem and progenitor cell enrichment kit (Cat# 558451, BD Biosciences). LSK cells were plated in X-Vivo hematopoietic cell medium (Cat# 12001-988(04-418Q), Lonza) supplemented with murine IL-3 (10ng/ml; Cat# 213-13, PeproTech), SCF (100ng/ml; Cat# 250-03, PeproTech), and human IL-6 (6ng/ml; Cat# 200-06, PeproTech) overnight to stimulate proliferation. LSK cells were transduced with pMIG-MLL-AF9-3xty1 (provided by Dr. Daisuke Nakada, Baylor College of Medicine) in 2 spinoculations using retronectin (Cat# T100B, Takara)-coated plates. Twenty-four hours after the second spinoculation, 200,000 cells containing ~10% transduced cells were transplanted to lethally irradiated (950 rads) C57BL/6J recipient mice. Moribund mice were humanely euthanized, and bone marrow cells were flushed from femur and tibia using PBS with 3% heat-inactivated FBS and counted using Cellometer Auto 2000 (Nexcelom). Bone marrow samples were analyzed by flow cytometry to confirm myeloid leukemic burden (~95% GFP-positive cells) and frozen in X-vivo medium with 10% DMSO.

**Leukemia detection.** Gating to select leukemic cells (GFP<sup>+</sup>) used the PE channel to control for autofluorescence. The gating strategy was developed based on non-leukemic GFP<sup>-</sup> control cells. For experiments in which the PE channel was used by a marker, the APC-Cy7 channel was used to control for autofluorescence.

### Supplemental Citations

1. Papillon JPN, Nakajima K, Adair CD, et al. Discovery of Orally Active Inhibitors of Brahma Homolog (BRM)/ SMARCA2 ATPase Activity for the Treatment of Brahma Related Gene 1 (BRG1)/SMARCA4-Mutant Cancers. *J Med Chem.* 2018;61(22):10155–10172.
2. Hodges HC, Stanton BZ, Cermakova K, et al. Dominant-negative SMARCA4 mutants alter the accessibility landscape of tissue-unrestricted enhancers. *Nat Struct Mol Biol.* 2018;25:61–72.
3. Kim D, Paggi JM, Park C, Bennett C, Salzberg SL. Graph-based genome alignment and genotyping with HISAT2 and HISAT-genotype. *Nat Biotechnol.* 2019;37(8):907–915.
4. Anders S, Pyl PT, Huber W. HTSeq—a Python framework to work with high-throughput sequencing data. *Bioinformatics.* 2015;31(2):166.
5. Love MI, Huber W, Anders S. Moderated estimation of fold change and dispersion for RNA-seq data with DESeq2. *Genome Biol.* 2014;15:550.
6. Korotkevich G, Sukhov V, Budin N, et al. Fast gene set enrichment analysis. *bioRxiv.* 2019;060012.
7. Lopez-Delisle L, Rabbani L, Wolff J, et al. pyGenomeTracks: reproducible plots for multivariate genomic datasets. *Bioinformatics.* 2021;37(3):422–423.